SUPPLEMENTARY INFORMATION

Slippery Wenzel State

Xianming Dai, Birgitt Boschitsch Stogin, Shikuan Yang, and Tak-Sing Wong

Department of Mechanical and Nuclear Engineering and Materials Research Institute, The Pennsylvania State University, University Park, PA 16802, USA

To whom correspondence should be addressed. Electronic address: tswong@psu.edu.

Supplementary Movies

Movie 1 shows a highly mobile water droplet, which impregnates the lubricated micropillars (Wenzel state). The droplet volume is 10 μL. The micropillar sizes are: w = 20 μm, L = 50 μm, h = 50 μm.

Movie 2 shows a mobile water droplet in Cassie state, moving on the tips of lubricated micropillars. Note that the Cassie state is metastable. The droplet volume is 10 μL. The micropillar sizes are: w = 20 μm, L = 50 μm, h = 50 μm.

Movie 3 shows a mobile hexadecane droplet in the Wenzel state that has a sliding angle of ~5^o on the lubricated rough surface. The volume of hexadecane droplet is 10 μL. The micropillar sizes are: w = 47 μm, L = 53 μm, h = 19 μm.

Movie 4 shows that by pressing the water droplet on the lubricated microstructures, a transition from the Cassie state to the Wenzel state is induced, but such a wetting transition does not hinder the drop mobility. Note that the Cassie state is metastable. The droplet volume is 10 μL. The micropillar sizes are: w = 20 μm, L = 50 μm, h = 50 μm.

SUPPLEMENTARY INFORMATION

Movie 5 shows that adding low surface tension liquids (ethanol) to a Cassie state water droplet induces the transition from Cassie state to Wenzel state but that the mobility of the mixture of water-ethanol droplet on the slippery rough surface is not hindered. Note that the Cassie state is metastable. The droplet volume is 10 μL. The micropillar sizes are: w = 20 μm, L = 50 μm, h = 50 μm.

Movie 6 shows hemi-wicking of a heptane droplet on the lubricated rough surface at roughness ~ 2.13. The volume of the heptane droplet is 5 μL. The micropillar sizes are: w = 15 μm, L = 15 μm, h = 17 μm.

1. Slippery Cassie State.

When a liquid droplet rests on top of a roughened surface and the droplet has not impregnated the surface textures but rather gas fills the textures, the droplet is in the Cassie state (Figure S1). Our substrates are hierarchically structured such that lubricant fills the nanostructures, while gas fills the microstructures, thus creating a conformal lubricant layer on the microstructures. We consider a liquid droplet that does not impregnate the microtextures to be in the Cassie state. We have demonstrated that our slippery rough surfaces still maintain high Cassie state droplet mobility on these lubricated rough surfaces (Figure S1). Note that the Cassie state is metastable.

SUPPLEMENTARY INFORMATION

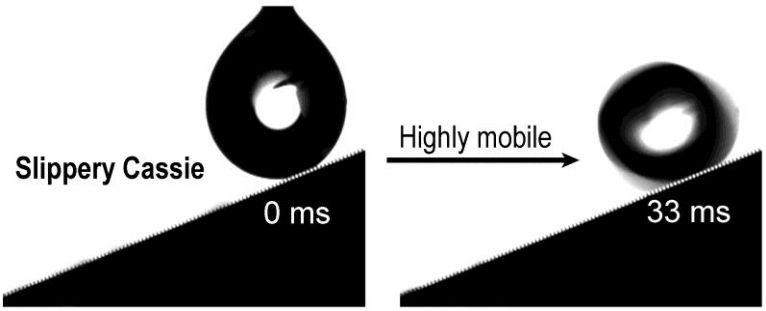

Figure S1. Slippery Cassie State (see Supplementary Movie S2).

2. Experimental Verification of Stable Lubricated Film Formation.

We conducted further analysis to show that conformal lubricant coating can be achieved on the microstructures for all solid-lubricant combinations against various contacting fluids investigated in this work. In order to form a thermodynamically stable lubricant layer within the nanotextures, the solid-lubricant combination should satisfy the following relationships [1,2]:

$$\Delta E_1 = r(\gamma_B \cos\theta_B - \gamma_A \cos\theta_A) - \gamma_{AB} > 0 \quad \text{(Eq. S1)}$$

$$\Delta E_2 = r(\gamma_B \cos\theta_B - \gamma_A \cos\theta_A) + \gamma_A - \gamma_B > 0 \quad \text{(Eq. S2)}$$

where r is the roughness of the nanotextures; γ_A and γ_B are, respectively, the surface tensions for the foreign liquid (Liquid A) and for the lubricant (Liquid B); γ_{AB} is the interfacial tension between the foreign liquid and lubricant; θ_A and θ_B are, respectively, the equilibrium contact angles (CAs) for the foreign liquid and the lubricant on a flat solid surface. The roughness of the nanotextures was estimated to be 14.6 ± 0.3 on the side of the micropillar and 19.3 ± 0.4 on the top of the micropillar through image analysis of high resolution scanning electron micrographs. These relationships dictate the solid-lubricant combinations that form an energetically stable lubricating film within the textured solid without being displaced by an external fluid. Our experimental measurements (Table S1) confirmed that the solid/lubricant/foreign liquid

SUPPLEMENTARY INFORMATION

combinations used in our experiments fulfilled the requirements outlined by Eqs. S1 and S2 (*i.e.*, $\Delta E_1 > 0$ and $\Delta E_2 > 0$).

Table S1. Theoretical and experimental verifications for the formation of the stable conformally lubricated microstructures

Solid	Liquid A	Liquid B	r	γ_A	γ_B	γ_{AB}	θ_A	θ_B	ΔE_1	ΔE_2	Stable?	
											Theory	Exp.
Silanized silicon	Water	Krytox 101	14.6	72.4	17.0	56.4	121.3	42.3	675.7	787.5	Y	Y
Silanized silicon	Glycerol	Krytox 101	14.6	60.1	17.0	40.5	122.6	42.3	615.6	699.2	Y	Y
Silanized silicon	Ethylene glycol	Krytox 101	14.6	48.2	17.0	28.1	112.4	42.3	423.5	482.8	Y	Y
Silanized silicon	Dipropylene glycol	Krytox 101	14.6	32.1	17.0	13.5	93.3	42.3	197.0	225.6	Y	Y
Silanized silicon	Hexadecane	Krytox 101	14.6	27.3	17.0	8.7	84.9	42.3	139.0	158.1	Y	Y
Silanized silicon	Undecane	Krytox 101	14.6	24.6	17.0	7.7	76.3	42.3	90.6	105.9	Y	Y
Silanized silicon	Ethanol	Krytox 101	14.6	21.1	17.0	8.3	76.4	42.3	102.6	115.0	Y	Y
Silanized silicon	Hydrid PDMS	Krytox 101	14.6	20.2	17.0	5.6	66.1	42.3	58.5	67.2	Y	Y
Silanized silicon	Heptane	Krytox 101	14.6	19.9	17.0	4.4	62.8	42.3	46.3	53.6	Y	Y

Note: "Silanized silicon" refers to nanotextured microstructures that were silanized by the heptadecafluoro-1,1,2,2- tetrahydrodecyltrichlorosilane. "Y" indicates that Liquid B can form stable conformally lubricated microstructures. γ_A and γ_B represent the surface tensions of Liquid A and Liquid B, respectively (Table S2). γ_{AB} represents the interfacial tension between Liquid A and Liquid B (Table S3). θ_A and θ_B are the static CAs on silanized flat silicon substrate (Table S4). Since higher surface roughness will enhance the lubricant stability, we used the lower bound roughness (*i.e.*, r = 14.6) for the surface energy calculations in Table S1.

Table S2. Measured Surface Tension for Various Polar and Non-Polar Liquids.

Liquids	Surface tension (mN/m)	Number of measurements
Water	72.4 ± 0.2	5
Glycerol	60.1 ± 0.5	5
Ethylene glycol	48.2 ± 0.3	5
Dipropylene glycol	32.1 ± 0.5	5
Hexadecane	27.3 ± 0.2	5
Undecane	24.6 ± 0.3	5
Ethanol	21.1 ± 0.3	5
Hydrid PDMS	20.2 ± 0.3	5
Heptane	19.9 ± 0.4	5
Krytox 101	17.0 ± 0.2	5

SUPPLEMENTARY INFORMATION

Table S3. Measured Interfacial Tension between Two Immiscible Liquids.

Liquid/Liquid	Interfacial tension (mN/m)	Number of measurements
Water/Krytox 101	56.4 ± 1.0	5
Glycerol/Krytox 101	40.5 ± 0.4	5
Ethylene glycol/Krytox 101	28.1 ± 0.2	5
Dipropylene glycol/Krytox 101	13.5 ± 0.6	5
Hexadecane/Krytox 101	8.7 ± 0.2	5
Undecane/Krytox 101	7.7 ± 0.3	5
Ethanol/Krytox 101	8.3 ± 0.4	5
Hydrid PDMS/Krytox 101	5.6 ± 0.2	5
Heptane/Krytox 101	4.4 ± 0.3	5

Table S4. Measured Static CAs of Various Liquids on Silanized Flat Silicon.

Solids	Liquids	Contact angle (degrees)	Number of measurements
Silanized flat silicon	Water	121.3 ± 0.9	5
Silanized flat silicon	Glycerol	122.6 ± 0.4	5
Silanized flat silicon	Ethylene glycol	112.4 ± 0.6	5
Silanized flat silicon	Dipropylene glycol	93.3 ± 0.7	5
Silanized flat silicon	Hexadecane	84.9 ± 0.4	5
Silanized flat silicon	Undecane	76.3 ± 0.5	5
Silanized flat silicon	Ethanol	76.4 ± 0.7	5
Silanized flat silicon	Hydrid PDMS	66.1 ± 0.6	5
Silanized flat silicon	Heptane	62.8 ± 0.3	5
Silanized flat silicon	Krytox 101	42.3 ± 0.5	5

SUPPLEMENTARY INFORMATION

3. Surface Morphology and Wetting Characteristics of the Hierarchical Micro/nano-Structured Surfaces before and after Lubrication.

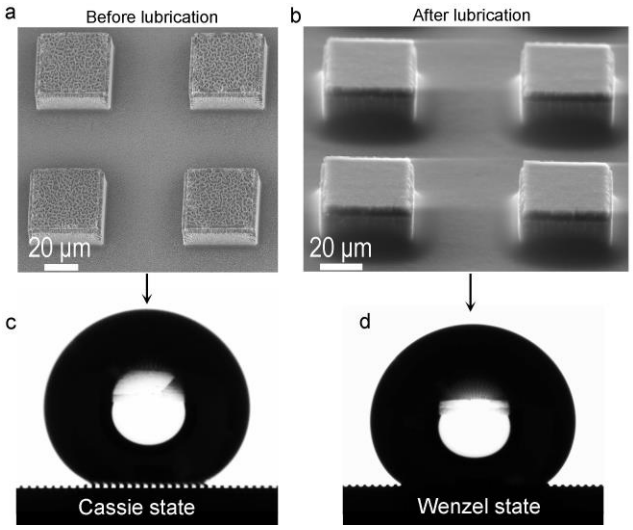

Figure S2. Wetting on hierarchical microstructured surfaces before and after lubrication. (a) SEM image of the hierarchical micro/nanostructures. (b) SEM image of the lubricated microstructures. (c) A Cassie state droplet on the hierarchical micro/nanostructures. (d) A Wenzel state droplet on the lubricated microstructures.

4. Wetting of Highly Wetting Liquids on Slippery Rough Surfaces Varying in Roughness.

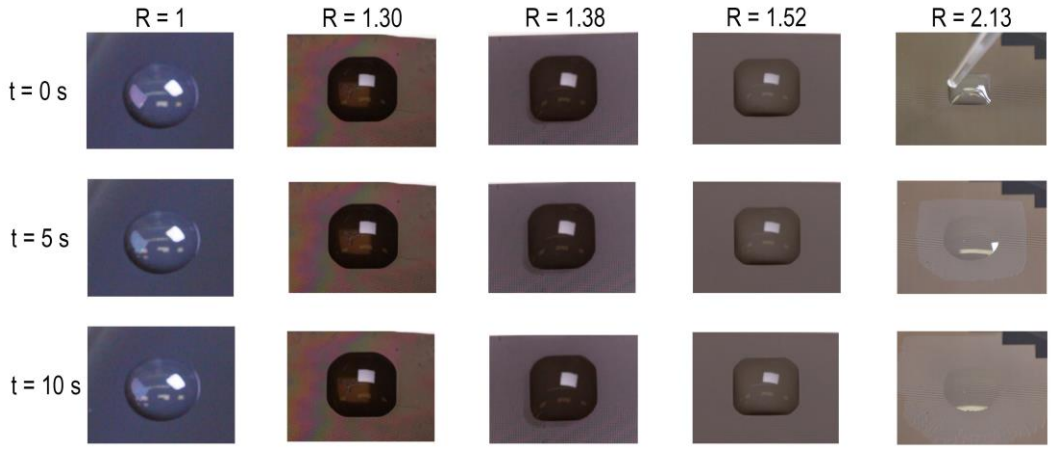

Figure S3. Wetting of heptane on slippery rough surfaces each with a different surface roughness. Notice that heptane droplets did not leave a wet footprint (a possible indicator of Wenzel state to hemi-wicking transition) or exhibit visible hemi-wicking on the lubricated rough surfaces at the surface roughness $R \leq 1.52$. At $R = 2.13$, heptane hemi-wicked the surface spontaneously (see Supplementary Movie S6).

SUPPLEMENTARY INFORMATION

5. Surface Morphology of Slippery Rough Surfaces Varying in Roughness.

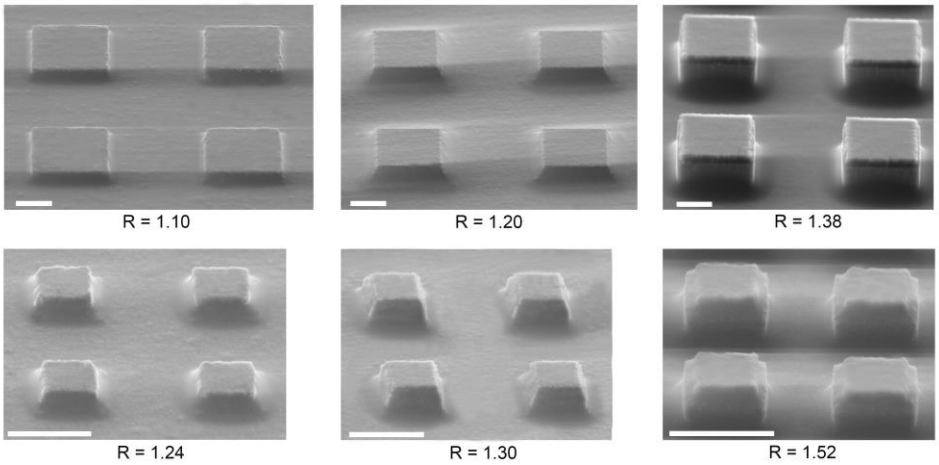

Figure S4. Environmental SEM images of lubricated rough surfaces varying in roughness *R*. Scale bars represent 20 μm.

6. Contact Angle (CA) and Sliding Angle on Lubricated Microstructures.

The sliding angle, CA, and CA hysteresis were measured by an automated contact angle goniometer (ramé-hart) at room temperature (21 – 24 ^{o}C) with ~20% relative humidity. The system was calibrated before the measurements were conducted. The image of the droplet was captured through a camera equipped with the optical system and the drop imaging software measured the CA, CA hysteresis, and the sliding angle.

In an effort to measure the CA under known and repeatable conditions, a lubrication protocol was established. As part of the protocol, we coated oil lubricant onto the nanotextured micropillars (w = 47 μm, L = 53 μm, h = 19 μm) at a spin speed of 8000 – 12000 rpm. The lubricant was trapped in the nanotextures, creating a surface with lubricated micropillars.

During the measurement, the stage was tilted automatically at the speed of 1 – 2 degrees/second and the drop image was captured every 0.5 to 1 second (faster tilting speeds were

used for more volatile droplet fluids). The sliding angle can be obtained by analyzing those images. When the contact line starts to move, the associated tilted angle is taken as the sliding angle. The accuracy of the measurement is ± 0.5^{o}. The measured sliding angles were used to estimate the droplet retention forces on the lubricated rough surfaces with different pillar heights (Figure S5).

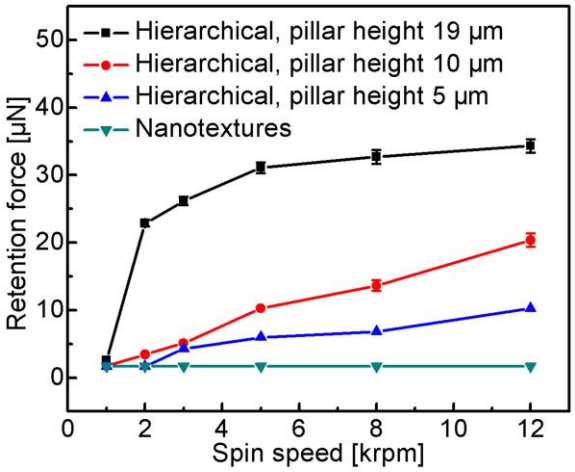

Figure S5. Retention forces of water droplets on the lubricated rough surfaces with different pillar heights. Error bars represent the standard deviation for three independent measurements.

7. Importance of Nanotextures for Lubricant Retention and Long Term Stability of the Slippery Rough Surfaces.

To demonstrate the importance of the nanotextures for lubricant retention, we compared the sliding angles on lubricated micropillars with and without nanostructures (Fig. S6). As illustrated in Fig. S6, it was observed that the nanotextures could significantly enhance the robustness and can maintain the slippery property even after continuous shedding of 200 droplets. However, without nanotextures, the lubricant cannot be well retained and can be removed by shedding of only 3 droplets. This further illustrates the importance of the nanostructures for lubricant

retention.

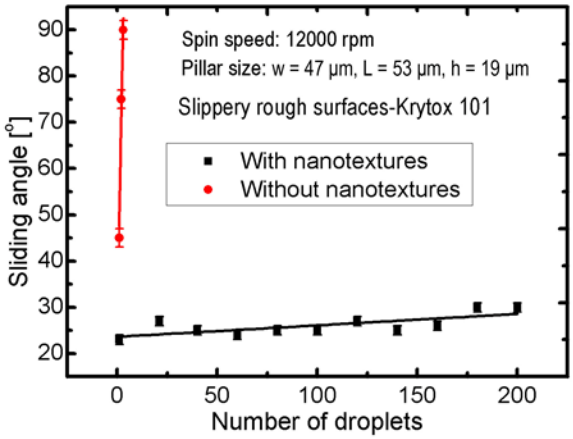

Figure S6. Sliding angle on lubricated micropillars with and without nanostructures. Error bars indicate standard deviation for at least 3 independent measurements.

8. Long Term Stability of the Perfluorinated Lubricants on Slippery Rough Surfaces.

There are two important factors that will influence the long-term stability of the lubricated rough surfaces: I) the miscibility of lubricant and the contacting fluid, and II) the evaporation rate of the lubricant. In order to enhance longevity for a given application, the lubricant should be chosen for its low miscibility and low evaporation rate. In our study, we chose perfluorinated lubricants since they are immiscible to both aqueous and non-aqueous liquids.

We further studied the evaporation rates of the perfluorinated lubricants infused into the slippery rough surfaces using a high-resolution analytical balance (Mettler Toledo XP504 DeltaRange, resolution = 0.1 mg). The lubricants under investigations include perfluorinated oils (*i.e.*, Krytox 101 and 103, DuPont). Krytox oils are fluorocarbon polymers of polyhexafluoropropylene oxide. There are Krytox oils with similar surface tensions (*i.e.*, ~ 17 – 18 mN/m) but with different viscosities, ranging from Krytox 100 to 107 with increasing

viscosity and boiling point. We have conducted experiments to monitor the evaporation of the lubricants under static, ambient conditions. We define the relative mass of lubricant, M^*, as the residual lubricant weight in the textures at an instant in time $M(t)$ normalized by the original lubricant weight M_0, *i.e.*, $M^* = M(t)/M_0$, where t is time. While the relative mass of Krytox 101 reduced by ~ 35% over the course of 15 days, our measurements showed that we could substitute the lubricant with Krytox 103 to minimize the effect of lubricant evaporation as this lubricant showed significantly reduced mass loss (~ 5 – 10%) during the same period of testing (Fig. S7).

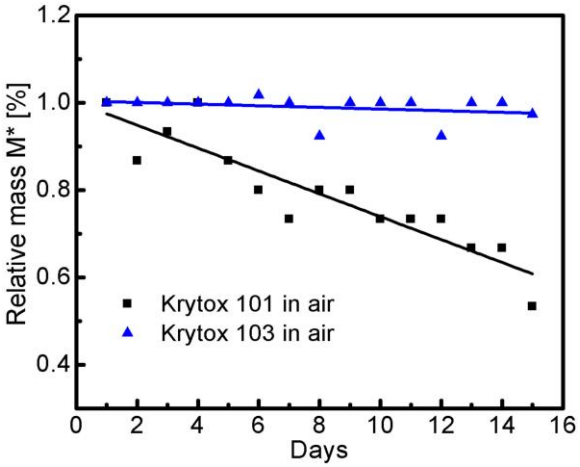

Figure S7. Evaporation effect on the lubricant loss of lubricated rough surfaces. Based on the instrumental resolution, the measurements errors were determined to be <10% of the measured M^* for all of these data.

To further study the effect of lubricant evaporation on the liquid repellency of the lubricated rough surfaces, we continued to study the drop mobility on the Krytox 101 and Krytox 103 lubricated rough surfaces (Fig. S8). Consistent with our lubricant evaporation data, the rough surfaces lubricated with Krytox 101 showed gradual degradation of liquid repellency over the course of 14-days as exhibited by the noticeable increase in the sliding angle (*i.e.*, an increase of 9

degrees). In comparison, the rough surfaces lubricated by Krytox 103 showed consistent liquid-repellency performance within our 14-days experimental time frame (*i.e.*, an increase of < 3 degrees). Our experimental data further supported that the longevity of slippery rough surfaces can be engineered by selecting appropriate lubricants for specific applications.

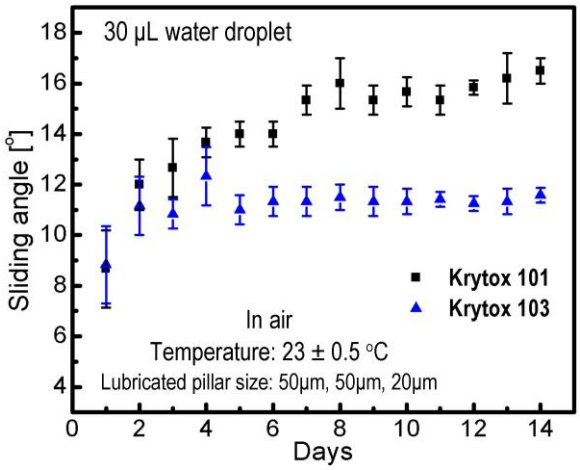

Figure S8. Effect of lubricant evaporation on the liquid repellency of the slippery rough surfaces lubricated with either Krytox 101 or 103. Error bars represent the standard deviation for three independent measurements.

References

1 Lafuma, A.; Quéré, D., Slippery pre-suffused surfaces. *Europhys. Lett.* **2011,** *96*, 56001.

2 Wong, T.-S.; Kang, S. H.; Tang, S. K. Y.; Smythe, E. J.; Hatton, B. D.; Grinthal, A.; Aizenberg, J., Bioinspired self-repairing slippery surfaces with pressure-stable omniphobicity. *Nature* **2011,** *477*, 443-447.